Rev. Roum. Sci. Techn.– Électrotechn. et Énerg.
Vol. **71**, *1*, pp. 163–168, Bucarest, 2026

MAGNETIC ANALYSIS OF ROTATING MAGNETIC FIELD DEVICES USED FOR STUDIES ON BLOOD CELLS

VALENTIN IONITA[1], MIHAI REBICAN[1], LUCIAN PETRESCU[1]

Keywords: Electrical engineering computing; Magnetic analysis; Magnetic cores; Rotating magnetic field; Biological cells.

The study of the molecular-level effects in blood cells of the variable magnetic field requires the design of appropriate magnetic devices. In this article, four immobile configurations are analyzed: Helmholtz coils, Gramme coils, a 4-pole electromagnet, and a 6-pole electromagnet. These devices can create a rotating magnetic flux density, intense (up to hundreds of mT), of high frequency (up to 1 MHz) and with an appropriate degree of inhomogeneity (maximum 5 %) in the bioreactor area of 1 cm in diameter. The rotating field is created by supplying the component coils with currents having shifted phases. The original comparative numerical analysis with the help of COMSOL software highlighted the effect of the device geometry, the type of core and conductor, correlated with the working frequency, on the magnetic flux density level in the blood cells. Original and useful results were extracted from the analysis of the homogeneity of the magnetic field in the bioreactor domain.

1. INTRODUCTION

The effects of magnetic flux density on biological cells have been intensively studied [1], but most scientific work refers to usual levels of tens of mT. Strong magnetic fields have been addressed in the field of particle acceleration (e.g., in [2]), but the main parameter is the field gradient, not the magnetic flux density level. In the case of a multipole electromagnet, ensuring a uniform field in the area of the biological sample requires a careful design of the poles so that the field lines do not close through the neighboring poles, but cross the sample. This problem has long been avoided by using coreless sources of uniform magnetic field, such as Helmholtz coils. The increased interest in biomedical studies in intense, rotating magnetic fields and at the highest possible frequencies has led to new core configurations being proposed: Gramme coils [3] or multipolar electromagnets [4–6].

Generators of the highest possible magnetic field, including pulsating ones, have been made using superconducting magnets. Thus, in [7] a system with three coaxial coils, powered by capacitor banks, is presented, which produces a pulsating unidirectional magnetic field with a peak value of 73.3 T. At the same time, an 85 T duplex magnet is detailed in [8], but the power supplies involved are of the order of gigawatts and do not provide a rotating field. In the field of magnetic resonance imaging (MRI), systems that produce constant magnetic fields of the order of 1.5-3 T are also optimized [9]. Pulsating electromagnets that produce pulses of 20 T and 3 ms are used in the study of materials [10]. The optimization of coils used in coreless generators of the Helmholtz, Merritt, or Maxwell type to obtain a uniform axial magnetic field is addressed in articles such as [11]-[14].

The original objective of our study was to find structures that do not involve superconductivity, are compact, and can be powered from a regular electricity network. These devices ensure a maximum and uniform level of magnetic flux density in the central area intended for the bioreactor containing living cells. In addition, the phase-shifted power supply of the coils ensures the production of a rotating magnetic field.

This study is focused on four configurations (Helmholtz coils, Gramme coils, 4-pole electromagnet, and 6-pole electromagnet) in which the coils are powered in such a way as to create a rotating field of the greatest possible amplitude in the area of interest occupied by blood cells placed in a 1 cm diameter cylindrical bioreactor. The geometry and the used materials were initially designed through the analytical optimization of the magnetic flux closure paths, to have uniformity in the bioreactor area and the necessary access space to it. The results of the magnetic analysis highlight the correlation between the magnetic core (geometry and materials), the coil conductor, the working frequency, and the level of magnetic flux density in the bioreactor with a degree of inhomogeneity of no more than 5%. This homogeneity was evaluated starting from the relative volume root mean square (rVRMS), used in magnetic resonance imaging (MRI) quality recommendations [15].

2. MAGNETIC FIELDS AND MOLECULAR EFFECTS

The effects of the magnetic field on living cells, both at the cellular and molecular levels, have been intensively studied over time. Initially, the research was carried out in a uniform, homogeneous magnetic field of approximately 10 mT to assess the influence of the ambient magnetic field on the human body. With the progress of laboratory platforms, it was found that the diffusion of active biological molecules or chemical substances through the membrane of biological cells is affected by the presence of intense magnetic fields.

For example, the exchange of hemoglobin and oxygen in blood cells is affected in the presence of ultra-high magnetic fields (50–100 T) [1]. The same effect also appears in the molecular diffusion associated with the injection of MRI contrast substances or anticancer drugs distributed locally with the help of paramagnetic nanoparticles. The studies presented in [16, 17] showed that the molecular diffusion in cells of paramagnetic or diamagnetic agents is influenced by the presence of sufficiently strong magnetic fields, even of short duration. The effects of cell lysis (breaking of cellular structures) can be like those caused by irradiation. Considering the temperature restrictions in the bioreactor, a solution is the use of superimposed magnetic pulses over moderate magnetic fields (up to 2 T).

Some experiments show that exposing biological cells to intense fields for short periods of time produces effects comparable to exposure to normal fields for longer periods, so an important factor is the total amount of energy transferred to the cells. The goal of our research is to

[1] Faculty of Electric Engineering, National University of Science and Technology POLITEHNICA Bucharest, Romania.
E-mails: valentin.ionita@upb.ro, mihai.rebican@upb.ro, lucian.petrescu@upb.ro

DOI: 10.59277/RRST-EE.2026.1.27

establish the limits of this hypothesis, which would allow to shorten the preliminary scientific experiments. The results presented in this article show how we can produce this homogeneous and rotating magnetic field, over which very short pulses (nanoseconds) of ultra-intense magnetic field can be superimposed; these magnetic pulses will be obtained in the center of a coil connected to a target irradiated with a high-power laser pulse.

3. DESIGNED DEVICES

Four magnetic flux density sources were considered to produce homogeneous fields in the working area (a cylinder having a 1cm diameter and a 1 cm height). Their structures were heuristically optimized, starting from the analytical methods for calculating the magnetic flux density (magnetic circuits, Biot-Savart-Laplace formula, average length of magnetic flux lines). Later, the respective structures were modeled in COMSOL Multiphysics and were tested for different frequencies, magnetic yoke materials, and conductor sections. The conductor section was correlated with the penetration depth corresponding to the frequency, the diameter being 1 mm for 400 Hz and 0.2 mm for 300 kHz.

3.1 HELMHOLTZ COILS

Two pairs of Helmholtz coils (Fig. 1) spaced at 3 cm and 6 cm, respectively, supplied with alternating current of variable frequency, with phases shifted by 90 degrees, were used to generate the rotating magnetic flux density. Each coil has 400 turns, and the copper conductor has a 1 mm diameter for a 400 Hz working frequency. The current is calibrated to 3 A for the outer coils and 1.66 A for the inner coils, to have a constant amplitude of the rotating magnetic field.

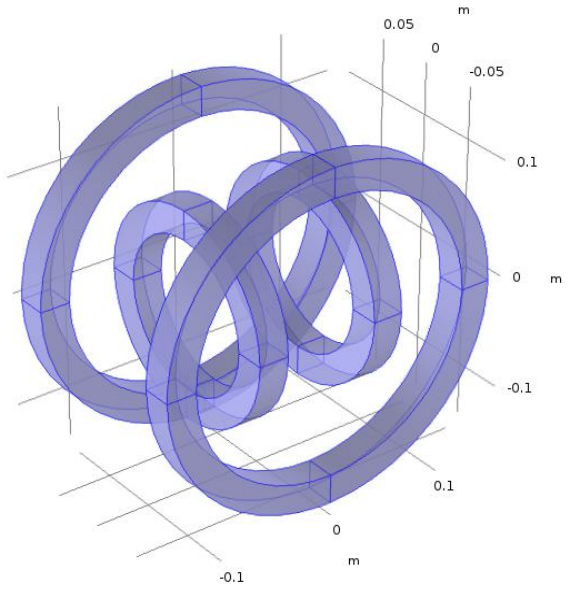

Fig. 1 – Structure of Helmholtz coils.

3.2 GRAMME COILS

The device shown in Fig. 2 has a square-shaped magnetic yoke with sides of 24 cm (outside) and 16 cm (inside), the thickness being 4 cm. The materials tested for the magnetic core were M-15 Steel (0.635 mm sheets) and Supermalloy (0.3 mm sheets). Each coil has 2400 turns, and the copper conductor has a 1 mm diameter for a 400 Hz working frequency, the current being 2 A. The four coils are supplied in such a way that a rotating magnetic flux density is generated in the middle area (occupied by the biological sample).

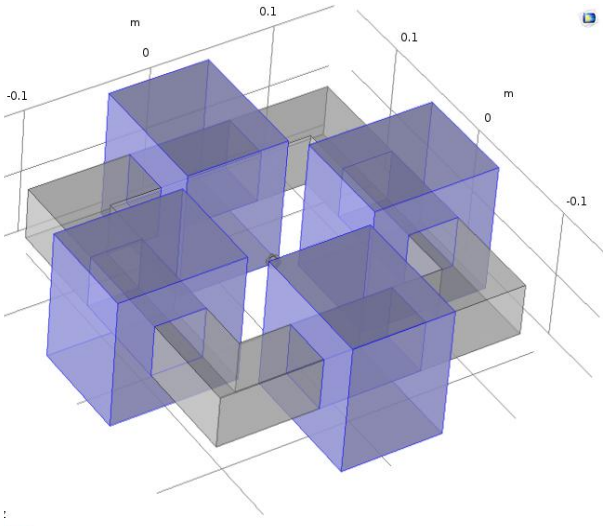

Fig. 2 – Geometry of Gramme coils.

3.3 ELECTROMAGNET WITH FOUR POLES

A 4-pole structure with two pairs of poles [18], commonly used in particle acceleration, was adopted to ensure magnetic flux density homogeneity in the middle area occupied by the bioreactor. The 4-pole electromagnet shown in Fig. 3 has two-section coils for optimal use of the core windows and to create a maximum field. The magnetic core, made of materials like those tested for Gramme coils, has a side of 22 cm and a thickness of 2 cm. The coils' power supply is two-phased, with a phase difference of 90 degrees to ensure the rotating field. Each coil has 1200 turns, and the copper conductor has a 1 mm diameter for a 400 Hz working frequency, the current being 3 A.

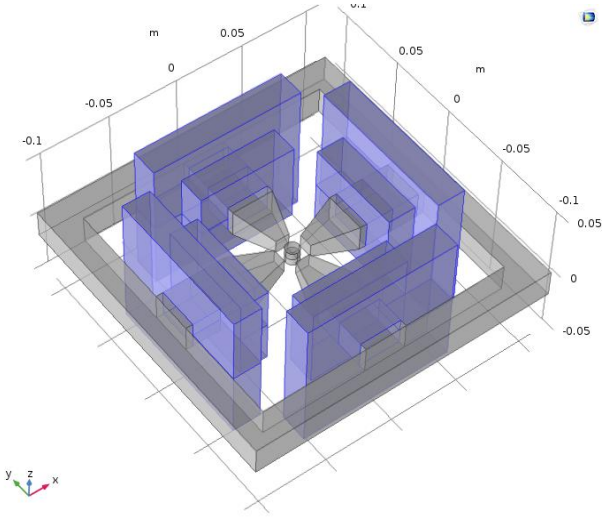

Fig. 3 – Optimized 4-pole electromagnet.

3.4 ELECTROMAGNET WITH SIX POLES

The fourth structure uses three pairs of poles with three-phase powered coils to generate a rotating magnetic flux density in the middle area occupied by the biological sample – see Fig. 4. For 400 Hz, each coil has 675 turns built by 1 mm diameter conductor, supplied by 3 A. For 300 kHz, one

used a Litz cable, each coil having 16000 turns made by 0.2 mm diameter conductor, the supplied current being 0.125 A.

The shape of the poles for the 4-pole and 6-pole electromagnets were iteratively corrected based on the analysis of the homogeneity of the magnetic field in the bioreactor area. Of course, an optimization based on genetic algorithms or other numerical tools could be applied for further improvements.

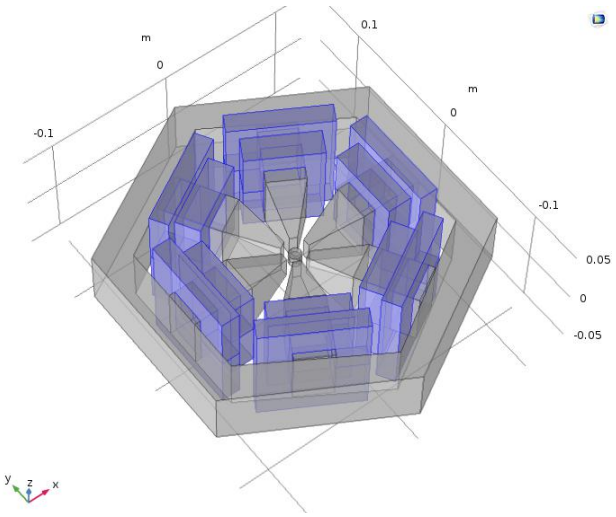

Fig. 4 – Optimized 6-pole electromagnet.

4. RESULTS OF NUMERICAL ANALYSIS

The numerical models of the four devices presented above were developed in the *COMSOL Multiphysics®* environment [19], which uses the finite element method to discretize the electromagnetic problem. The geometric model was built for the entire device, not taking advantage of existing symmetries, for possible later export to build the physical prototype. The objective of our study was to establish the limits of use of each source, always considering minimizing the losses in the core and conductors, in order to be able to use available sources to power the coils. The devices have been designed to operate without cooling, with a maximum current density of 4 A/mm^2 in the effective cross-section of the conductors, but a detailed thermal study could impose water cooling. Considering the voltage limitation of the usual signal amplifiers, for higher frequencies, series-parallel power supply schemes or even separate sources for the coils with more sections can be used.

Obviously, the structures with a magnetic core ensure higher values of the magnetic flux density produced, but the existence of the large air gap, necessary for placing the bioreactor, and the very high core losses limit the frequency range. Therefore, our tests focused on the frequency of 400 Hz, considered as a limit for the use of FeSi sheets in the core. Composite materials or ferrites used at higher frequencies do not give suitable results for these large air gap structures, due to the low saturation magnetization, which limits the value of the magnetic flux density in the air gap. It should be noted that all simulations are performed without saturating the cores.

The comparison of the four solutions for generating the rotating magnetic field considered three parameters:

a) The average value of the magnetic flux density modulus in the bioreactor - B_{med}.

b) The inhomogeneity factor in the central cross-section of the bioreactor - *IH* - defined as:

$$IH[\%] = \frac{100}{B_{xy}(\mathrm{O})} \sqrt{\frac{1}{A}\int_A \left(B_{xy}(\mathrm{P}) - B_{xy}(\mathrm{O})\right)^2 \mathrm{d}A} \qquad (1)$$

where B_{xy}(P) and B_{xy}(O) are the projections of the magnetic flux density on the $z = 0$ plane, at an arbitrary point P(x,y) and the center O of the cross-section of area A of the cylindrical bioreactor having a diameter of 1 cm.

c) The power supply efficiency - *PSE* - defined by the ratio between B_{med} and the current through the coil turns.

4.1 HELMHOLTZ COILS

The Helmholtz coil assembly produces, as expected, a uniform magnetic field (Fig. 5) that extends well outside the bioreactor area. The magnetic flux density level in the bioreactor is however low (B_{med} = 30 mT), with an extremely low inhomogeneity (*IH* = 0.4 %) and a power supply efficiency *PSE* = 10 mT/A for the working frequency of 400 Hz. The absence of the magnetic core allows the use of this magnetic source at higher frequencies, with the appropriate adaptation of the conductor section, but the level of the produced magnetic flux density remains as low. In addition, at kHz frequencies, the impedance of the coils increases greatly, and the current that can be injected by the signal amplifier is more limited; the value of B_{med} decreases substantially with increasing frequency.

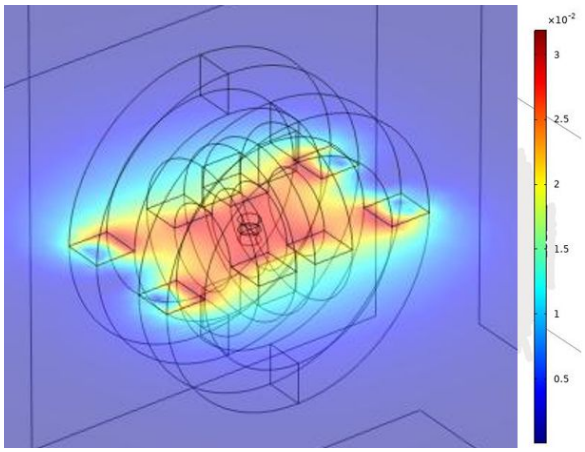

Fig. 5 – Magnetic flux density (in T) for Helmholtz coils at 400 Hz.

4.2 GRAMME COILS

The Gramme coils on the parallel branches of the magnetic core are energized to produce magnetic fields that cancel each other in the core and are added in the inner window. The laminated core made of M-15 sheets with a thickness of 0.635 mm was modeled as a homogeneous core characterized by an effective electrical conductivity [20, 21] that gives rise to the pseudo-skin effect in the core (see Fig. 6) but does not influence the field values outside the core. At 400 Hz, the magnetic flux density remains sufficiently homogeneous in the bioreactor (see Fig. 7), obtaining B_{med} = 48.4 mT at an inhomogeneity IH = 1 % in the central cross-section. For the vertical direction, it is observed that the homogeneity is even better, since the core thickness of 4 cm is greater than the height of 1 cm of the cylindrical bioreactor. The power supply efficiency is PSE = 24.2 mT/A, higher than that of Helmholtz coils, but the source will also

have to cover the core losses.

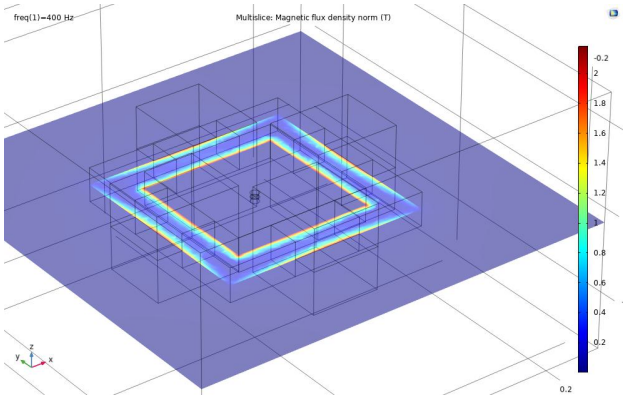

Fig. 6 – Magnetic flux density (in T) for the laminated core (M-15 sheets) of Gramme coils at 400 Hz.

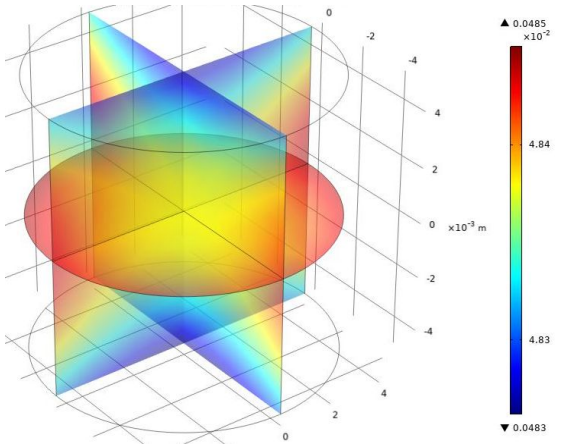

Fig. 7 – Distribution of magnetic flux density (in T) in the bioreactor, for Gramme coils at 400 Hz.

4.3 ELECTROMAGNET WITH FOUR POLES

The quadrupolar electromagnet was tested at 400 Hz, both for the M-15 sheet core and for the Supermalloy core. The distribution of magnetic flux density in the M-15 core is shown in Fig. 8, the magnetic material being unsaturated. On the other hand, for the Supermalloy core and the same coil supply, the numerical procedure for solving the electromagnetic problem did not converge, probably due to the rapid saturation of the core. For higher frequencies (300 kHz), the result was similar, requiring a consistent decrease in the current to avoid core saturation, but at the cost of a decrease to low values (below 100 mT) of the magnetic flux density in the bioreactor.

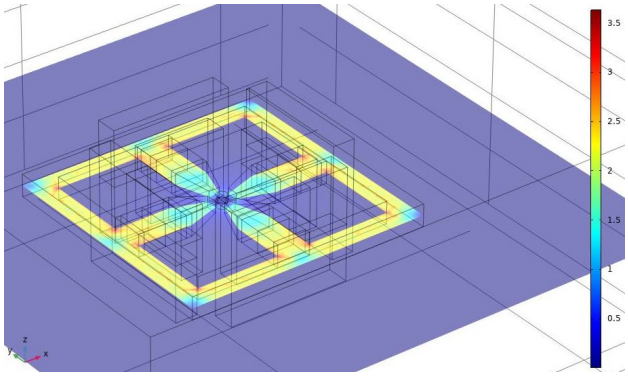

Fig. 8 – Distribution of magnetic flux density (in T) inside the core (M-15 sheets) of 4-pole electromagnet at 400 Hz.

The distribution of magnetic flux density in the central section of the bioreactor, for the M-15 sheet core at a frequency of 400 Hz, is shown in Fig. 9. It is worth noting the high value of the average magnetic induction (B_{med} = 480 mT) and the low inhomogeneity IH = 1.6%, although slightly higher than for the previous two configurations. The power supply efficiency is also superior (PSE = 160 mT/A), the two sections of each coil being able to be powered in series or parallel, depending on the available sources.

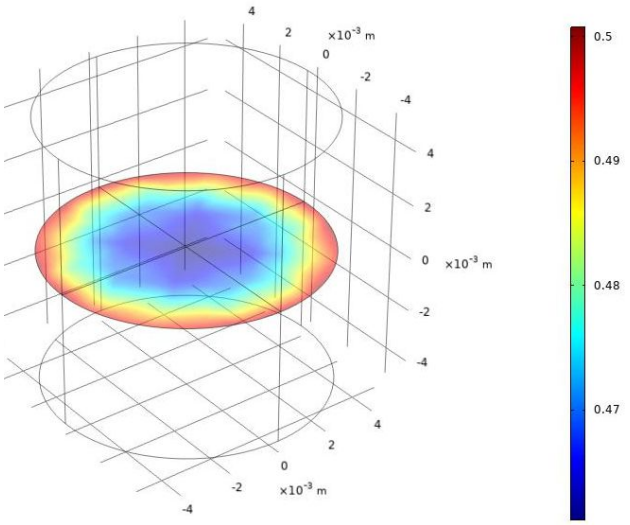

Fig. 9 – Distribution of magnetic flux density (in T) for the central section of the bioreactor placed in the 4-pole electromagnet, at 400 Hz.

4.4 ELECTROMAGNET WITH SIX POLES

The 6-pole electromagnet was numerically analyzed similarly to the 4-pole electromagnet. The greater proximity of each pole to the neighboring poles causes a greater dispersion of the magnetic field in the central air gap, the effect being more pronounced for the Supermalloy core used at 300 kHz. In this case, the core is only superficially saturated (Fig. 10), but the level of magnetic flux density in the bioreactor is reduced to B_{med} = 206 mT, with an inhomogeneity IH = 4.1 % (see Fig. 11). The behavior is similar at the frequency of 400 Hz, for the M-15 core (see Fig. 12): B_{med} = 230 mT (compared to 480 mT for the 4-pole electromagnet), but with a better homogeneity (IH = 2.8%).

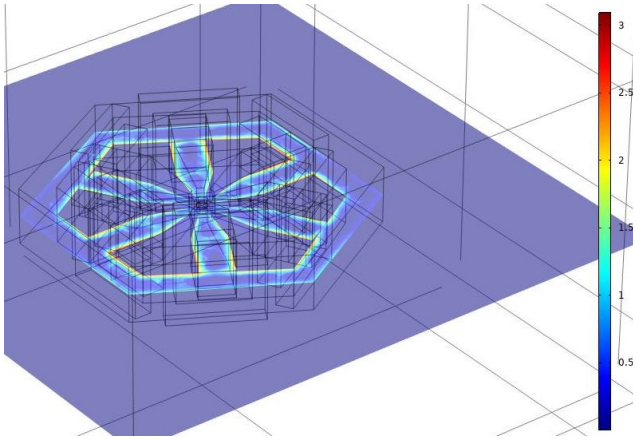

Fig. 10 – Magnetic flux density (in T) for the Supermalloy core of 6-pole electromagnet at 300 kHz.

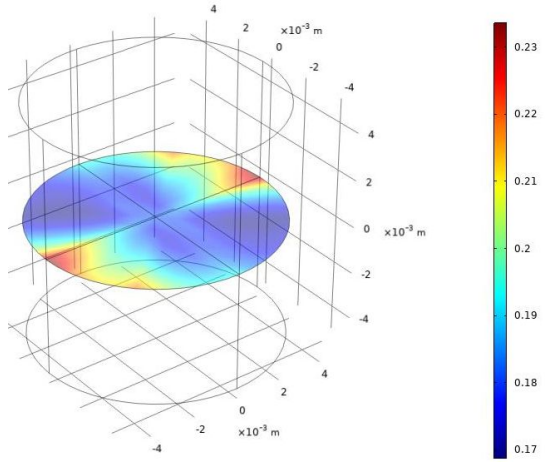

Fig. 11 – Distribution of magnetic flux density (in T) in the bioreactor, for 6-pole electromagnet with Supermalloy core at 300 kHz.

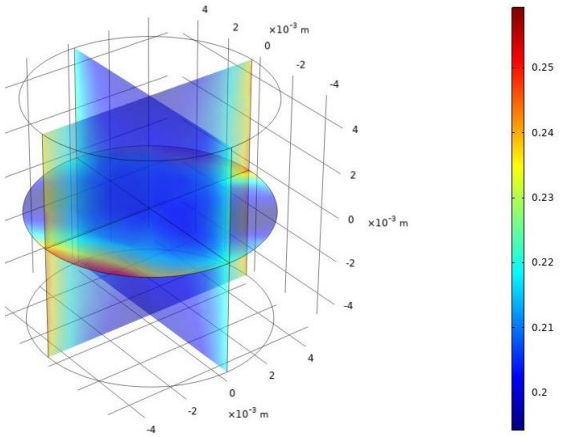

Fig. 12 – Distribution of magnetic flux density (in T) in the bioreactor, for 6-pole electromagnet with M-15 core at 400 Hz.

The numerical simulations were performed with the help of the COMSOL Multiphysics software, having the discretization mesh with hundreds of thousands of finite elements of the first order. For example, the discretization mesh from the area of the cylindrical bioreactor placed in the central space of the 6-pole electromagnet is presented in Fig. 13.

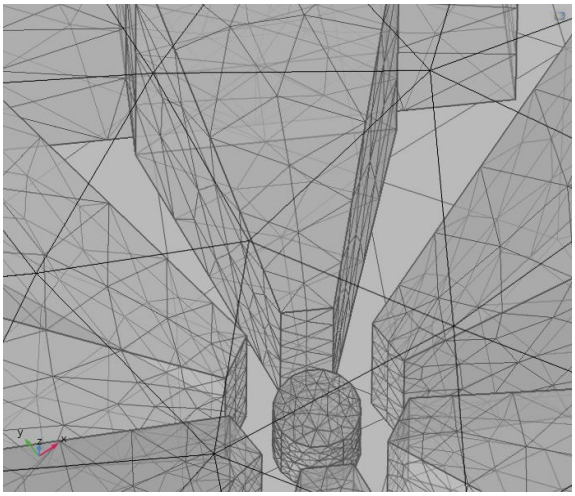

Fig. 13 – Mesh in the region of the bioreactor, placed in the central space of the 6-pole electromagnet (the entire mesh has 197050 finite elements).

The rotating magnetic field in the bioreactor is obtained by the appropriate phase shift of the supply currents through the pairs of coils. Thus, this phase shift is 90 degrees for the Helmholtz coils, the Gramme coils and the 4-pole electromagnet, while the 6-pole electromagnet is three-phase powered (120-degree phase shift). Numerical simulations confirmed this rotation of the magnetic flux density vector, while the distribution of its norm does not change, as can be seen in Fig. 14 for the electromagnet with 6 poles and M-15 core, at 400 Hz. Both good homogeneities can be observed, the norm of B being in the range (0.2 T – 0.25 T), and the weak but persistent effect of the neighboring pole (at 60 degrees) on this homogeneity, due to the diversion of some of the magnetic flux lines through the high magnetic permeability material of the neighboring pole.

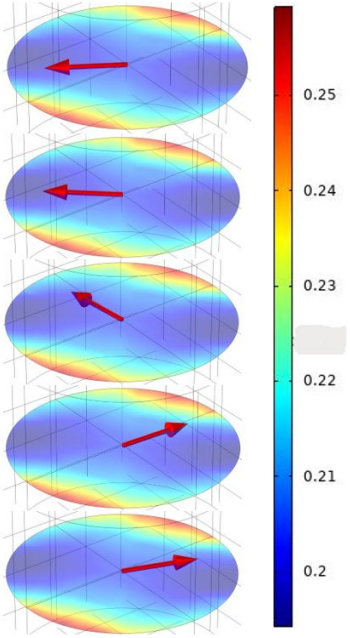

Fig. 14 – Rotation of the magnetic flux density vector in the central section of the bioreactor for the 6-pole electromagnet and M-15 core, at 400 Hz. The initial phase of the three-phase current is varied by 30 degrees from 0 (up) to 120 degrees (down).

5. **CONCLUSIONS**

This study presents optimized solutions for producing a homogeneous and rotating magnetic field in a limited area (cylinder with a diameter of 1 cm and a height of 1 cm), which does not require special cooling or power supply restrictions. The four designed devices can be used in biomedical experiments according to the magnetic field parameters highlighted in Section IV. Thus, the presented Helmholtz coils and Gramme coils can produce rotating magnetic fields with a magnetic flux density modulus below 50 mT, with a very low degree of inhomogeneity (below 1%). The proposed inhomogeneity indicator IH allows a good global assessment of the magnetic field conditions to which the studied biological cells are exposed.

Higher values of magnetic flux density in the bioreactor were accessible for multipolar electromagnets, the best

constructive solution being the 4-pole electromagnet, for which 480 mT at 400 Hz were obtained, compared to 230 mT for the 6-pole electromagnet. The working frequency can be increased if appropriate magnetic materials (amorphous, composite, ferrite) for the electromagnet core and Litz-type windings are used, but a detailed thermal calculation is necessary. The reactances of the coils can be minimized by compensation schemes with capacitor banks.

The study highlighted the different dependence, for each device, of the magnetic flux density distribution in the bioreactor depending on the core material and frequency – see Figs. 5, 7, 9, 11, 12, and 14. In addition to the low inhomogeneity in the reactor (1.6 % for the 4-pole electromagnet and 2.8 % for the 6-pole one), the presented distributions are also useful for predicting the degree of mixing of mobile biological cells under the action of the magnetic field, especially in the case of cells marked with magnetic nanoparticles.

The final technical decision regarding the use of one of the designed devices must also consider the sources available for the phase-shifted power supply of the coils. The design of each coil with several sections allows the use of multiple and modular power sources.

ACKNOWLEDGMENT

This work has been funded by the National Project PNCDI IV/P5.9/5.9.1/ELI-RO no. 30/2024 “Effects of ultra-intense transient magnetic fields, generated by high-power lasers, on leukemic and lymphomatous cancer cells / HiPoCell.”

CREDIT AUTHORSHIP CONTRIBUTION STATEMENT

Valentin Ionita: conceptualization, investigation, writing - original draft
Mihai Rebican: 3D numerical simulation, writing – review
Lucian Petrescu: investigation, preliminary 2D numerical simulation

Received on 27 January 2026

REFERENCES

1. M. Tota, L. Jonderko, J. Witek, V. Novickij, J. Kulbacka, *Cellular and molecular effects of magnetic fields*, International Journal of Molecular Sciences, **25**, *16*, 8973 (2024).
2. S. Prawanta, P. Sunwong, B. Boonwanna, V. Sooksrimuang, A. Kwankasem, S. Pongampai, P. Sudmuang, P. Klysubun, *Design and construction of sextupole magnet prototype for Siam Photon Source II*, 10th International Particle Accelerator Conference (IPAC 2019), Melbourne, Australia, pp. 4285–4297 (2019).
3. A. Skumiel, J. Musiał, *The use of Gramme coils in a 2-phase system for generation of a high frequency rotating magnetic field*, Journal of Magnetism and Magnetic Materials, **564**, 170198 (2022).
4. N. Hallali, T. Rocacher, C. Crouzet, J. Béard, T. Douard, A. Khalfaoui, *Low-frequency rotating and alternating magnetic field generators for biological applications: design details of home-made setups*, Journal of Magnetism and Magnetic Materials, **564**, 170093 (2022).
5. A. Skumiel, *Generation of a rotating high frequency magnetic field designed for use in magnetic hyperthermia*, Journal of Magnetism and Magnetic Materials, **553**, 169294 (2022).
6. R.M. Wojciechowski, A. Skumiel, M. Kurzawa, A. Demenko, *Design, application and investigation of the system for generation of fast changing, rotating magnetic field causing hyperthermic effect in magnetic liquids*, Measurement, **194**, 111020 (2022).
7. H. Ding, Z. Zhao, C. Jiang, Y. Xu, T. Ding, X. Fang, T. Ren, L. Li, Y. Pan, T. Peng, *Construction and test of three-coil magnet power supply system for a high-pulsed magnetic field*, IEEE Transactions on Applied Superconductivity, **28**, *3*, 5000606 (2018).
8. J.R. Michel, S.B. Betts, J.D. Lucero, A. Bhardwaj, L.N. Nguyen, D.N. Nguyen, *Design and construction of the new 85 T duplex magnet at NHMFL–Los Alamos*, IEEE Transactions on Applied Superconductivity, **34**, *5*, 4900305 (2024).
9. Y. Song, Z. Cheng, X. Jiang, J. Li, L. Li, Q. Wang, *Design, test, and shimming of a 1.5 T head-only MRI superconducting magnet*, IEEE Transactions on Applied Superconductivity, **35**, *6*, 3800505 (2025).
10. I. Dobrin, D. Enache, G. Dumitru, M. Gutu, S. Zamfir, R. Pintea, *Curved dipolar electromagnet, numerical modeling and design*, Rev. Roum. Sci. Techn. – Électrotechn. et Énerg., **67**, *4*, pp. 409–415 (2022).
11. Y. Lu, Y. Yang, M. Zhang, R. Wang, L. Jiang, B. Qin, *Improved square-coil configurations for homogeneous magnetic field generation*, IEEE Transactions on Industrial Electronics, **69**, *6*, pp. 6350–6360 (2022).
12. Z. Ding, Z. Huang, M. Pang, G. Bai, Q. Wang, B. Han, *Optimized design of uniform-field coils system with a large uniform region by particle swarm optimization algorithm*, Measurement, **234**, 114614 (2024).
13. X. Zhu, C. Liu, H. Su, Y. Miao, H. Cheng, *Design of improved four-coil structure with high uniformity and effective coverage rate*, Heliyon, **9**, *4*, e15193 (2023).
14. O. Sucre, S. Glöggler, *Optimization method based on zonal harmonics for axially symmetric magnets*, IEEE Transactions on Magnetics, **61**, *2*, 5100109 (2025).
15. T.J. Havens, T. Duby, J. Huang, *VRMS homogeneity definition: a proposal*, Proceedings of the International Society for Magnetic Resonance in Medicine, Scientific Meeting and Exhibition (2002).
16. V. Zablotskii, T. Polyakova, A. Dejneka, *Effects of high magnetic fields on the diffusion of biologically active molecules*, Cells, **11**, *1*, 81 (2021).
17. C.M. Ciocazeanu, D.E. Nitescu, M. Morega, *Useful assumption for simplified numerical analysis of transcranial magnetic stimulation*, Rev. Roum. Sci. Techn. – Électrotechn. et Énerg., **70**, *3*, pp. 427–432 (2025).
18. L. Petrescu, V. Ionita, M. Rebican, M.C. Petrescu, *Optimization of quadrupole core for homogenous magnetic field using non-oriented silicon-iron materials*, U.P.B. Scientific Bulletin, Series C, **87**, *4* (2025).
19. ***COMSOL, *COMSOL Multiphysics® modeling software*.
20. A. Bermudez, D. Gomez, P. Salgado, *Eddy-current losses in laminated cores and the computation of an equivalent conductivity*, IEEE Transactions on Magnetics, **44**, *12*, pp. 4730–4738 (2008).
21. F. Saftoiu, Y. Veli, A.M. Morega, *Electropermeabilization for organic material – numerical modeling*, Rev. Roum. Sci. Techn. – Électrotechn. et Énerg., **70**, *4*, pp. 603–608 (2025).